Available online at www.sciencedirect.com
SCIENCE DIRECT
Biochimica et Biophysica Acta 1758 (2006) 336–346
BIOCHIMICA ET BIOPHYSICA ACTA
BBA
http://www.elsevier.com/locate/bba

Cellular uptake of $S4_{13}$-PV peptide occurs upon conformational changes induced by peptide–membrane interactions

Miguel Mano [a,b], Ana Henriques [c], Artur Paiva [c], Manuel Prieto [d], Francisco Gavilanes [e], Sérgio Simões [a,f], Maria C. Pedroso de Lima [a,b,*]

[a] *Centro de Neurociências e Biologia Celular, Universidade de Coimbra, Portugal*
[b] *Departamento de Bioquímica, Faculdade de Ciências e Tecnologia, Universidade de Coimbra, Portugal*
[c] *Centro de Histocompatibilidade de Coimbra, Portugal*
[d] *Centro de Química-Física Molecular, Instituto Superior Técnico, Lisboa, Portugal*
[e] *Departamento de Bioquímica y Biologia Molecular I, Facultad de Ciencias Químicas, Universidad Complutense de Madrid, Spain*
[f] *Laboratório de Tecnologia Farmacêutica, Faculdade de Farmácia, Universidade de Coimbra, Portugal*

Received 29 September 2005; received in revised form 16 January 2006; accepted 18 January 2006
Available online 10 February 2006

Abstract

In face of accumulated reports demonstrating that uptake of some cell-penetrating peptides occurs through previously described endocytic pathways, or is a consequence of cell fixation artifacts, we conducted a systematic analysis on the mechanism responsible for the cellular uptake of the $S4_{13}$-PV karyophilic cell-penetrating peptide. The results reviewed here show that the $S4_{13}$-PV peptide is able to very efficiently accumulate inside live cells in a rapid, non-toxic and dose-dependent manner, through a mechanism distinct from endocytosis. Comparative analysis of peptide uptake by mutant cells lacking heparan sulfate proteoglycans demonstrates that, although not mandatory, their presence at cell surface facilitates the cellular uptake of the $S4_{13}$-PV peptide. Furthermore, we demonstrate that upon interaction with lipid vesicles, the $S4_{13}$-PV peptide undergoes significant conformational changes that are consistent with the formation of helical structures. Such conformational changes occur concomitantly with a penetration of the peptide into the lipid bilayer, strongly suggesting that the resulting helical structures are crucial for the non-endocytic cellular uptake of the $S4_{13}$-PV peptide. Overall, our data support that, rather than endocytosis, the cellular uptake of the $S4_{13}$-PV cell-penetrating peptide is a consequence of its direct translocation through cell membranes following conformational changes induced by peptide–membrane interactions.

Keywords: Cell-penetrating peptide; Protein transduction domain; Peptide–membrane interaction; Tryptophan fluorescence; Circular dichroism; Amphipathic alpha-helix

1. Introduction

Cell-penetrating peptides (CPPs) have been shown to very efficiently cross eukaryotic cell membranes through a temperature-insensitive and energy-independent mechanism that does not involve membrane receptors or transporters. Interestingly, cell-penetrating peptides also have the remarkable ability to mediate the intracellular delivery of a wide variety of molecules of pharmacological interest, both in vitro and in vivo (for recent reviews, see [1–5]).

Despite great variability in the amino acid sequence, CPPs are usually short peptide sequences rich in basic amino acids, in some cases exhibiting the ability to be arranged in amphipathic alpha-helices. The peptides derived from the HIV-1 Tat protein and from the homeodomain of the Antennapedia protein of *Drosophila* (Tat and Penetratin (pAntp) peptides, respectively) [6,7], as well as the synthetic Pep-1 peptide [8] are among the best-characterized cell-penetrating peptides.

Abbreviations: CPP, cell-penetrating peptide; GAG, glycosaminoglycan; HSPG, heparan sulfate proteoglycan; LUV, large unilamellar vesicle; POPC, 1-palmitoyl-2-oleoyl-*sn*-glycero-3-phosphocholine; POPG, 1-palmitoyl-2-oleoyl-*sn*-glycero-3-[phospho-*rac*-(1-glycerol)]; CD, circular dichroism

* Corresponding author. Departamento de Bioquímica, Faculdade de Ciências e Tecnologia, Universidade de Coimbra, Apartado 3126, 3001-401 Coimbra, Portugal. Tel.: +351 239820190; fax: +351 239853607.
E-mail address: mdelima@ci.uc.pt (M.C. Pedroso de Lima).

0005-2736/$ - see front matter © 2006 Elsevier B.V. All rights reserved.
doi:10.1016/j.bbamem.2006.01.014

Consistent with the capacity of CPPs and of their conjugates to enter into a wide variety of cell types from different tissues and organisms, the glycosaminoglycan (GAG) moieties of the ubiquitous cell surface heparan sulfate proteoglycans (HSPGs) have been identified as playing an important role in mediating electrostatic interactions of cell-penetrating peptides with biological membranes [9,10].

Despite the widespread use of cell-penetrating peptides for delivery purposes and the extensive research on the unusual ability of these peptides to traverse cell membranes and promote intracellular uptake of various cargo molecules, the mechanisms underlying the cellular uptake of CPPs are not completely elucidated. Recent reports attributing the cellular uptake and nuclear accumulation of some cell-penetrating peptides to an artifactual redistribution of membrane-associated peptide molecules and conjugates [11–13], have motivated a re-evaluation of the mechanisms responsible for their cellular uptake. Interestingly, results from criterious re-evaluations of cellular uptake under experimental conditions that avoid artifactual observations, have implicated the involvement of well-characterized endocytic pathways, such as clathrin-mediated endocytosis [10], caveolae-mediated endocytosis [14,15] or macropinocytosis [16,17] in the internalization of several peptides and their conjugates.

Given the conflicting results regarding the mechanisms on the cellular uptake of cell-penetrating peptides, we have previously characterized the cellular uptake of the $S4_{13}$-PV karyophilic cell-penetrating peptide [18]. In the present manuscript, we review research results obtained in our laboratory on the interaction of $S4_{13}$-PV peptide with cells and model membranes, aimed to understand the sequence of events underlying translocation of this peptide across biological membranes. The $S4_{13}$-PV cell-penetrating peptide results from the combination of a 13 amino acid cell-penetrating sequence, derived from the Dermaseptin S4 peptide, with the SV40 large T antigen nuclear localization signal [19]. Table 1 compares the amino acid sequence of the $S4_{13}$-PV peptide with those of cell-penetrating peptides commonly used for cargo delivery.

Collectively, the obtained data indicate that the cellular uptake of the $S4_{13}$-PV peptide is a very efficient, non-toxic and dose-dependent process, which occurs mainly through a mechanism distinct from endocytosis, most likely involving the direct penetration of the peptide through cell membranes.

Table 1
Comparison of the sequences of the $S4_{13}$-PV, reverse NLS and scrambled peptides, used in this study, with those of well-characterized cell-penetrating peptides

Peptide	Sequence	Reference
pAntp	RQIKIWFQNRRMKWKK	[7]
Tat	YGRKKRRQRRR	[6]
Pep-1	KETWWETWWTEWSQPKKKRKVC-NH_2	[8]
$S4_{13}$-PV	ALWKTLLKKVLKAPKKKRKVC-NH_2	[19]
reverse NLS	ALWKTLLKKVLKAVKRKKKPC-NH_2	
scrambled	KTLKVAKWLKKAKPLRKLVKC-NH_2	

SV40 large T antigen nuclear localization signal is underlined in the sequence of Pep-1, $S4_{13}$-PV and reverse NLS peptides; in the reverse NLS peptide, the sequence corresponding to the NLS of SV40 (aa 14–20) is inverted.

Comparative analysis of peptide uptake by mutant cells lacking heparan sulfate proteoglycans, as well as studies with model membranes, demonstrate that the presence of HSPGs or other negatively charged components on the surface of target membranes potentiates the extent of peptide–membrane interactions, which are mainly of electrostatic nature. As a consequence of these peptide–membrane interactions, the $S4_{13}$-PV peptide becomes inserted into the lipid bilayer, which occurs concomitantly with significant conformational changes of the peptide that are consistent with an increase in its helical content. Comparative analysis using different peptides demonstrates that these conformational changes are dependent on the peptide sequence, providing clear evidence that the secondary structure acquired by the $S4_{13}$-PV peptide upon its interaction with target membranes is intricately related to its capacity to translocate across cell membranes.

2. Materials and methods

2.1. Cells

HeLa cells (human epithelial cervical carcinoma) were maintained at 37 °C, under 5% CO_2, in Dulbecco Modified Eagle medium-high glucose (DMEM; Sigma, St. Louis, MO) supplemented with 10% (v/v) heat-inactivated fetal bovine serum (Biochrom KG, Berlin, Germany), and with 100 units penicillin and 100 μg streptomycin (Sigma) per ml.

CHO-K1 and pgs A-745 Chinese hamster ovary cell lines were grown in F-12 (Ham) Nutrient Mixture (Invitrogen, UK) supplemented with 10% fetal bovine serum, penicillin (100 units/ml) and streptomycin (100 μg/ml), 2 mM L-glutamine (Sigma), 10 mM HEPES (Sigma) and 14 mM sodium bicarbonate (Sigma).

2.2. Peptides

High purity (>95%) $S4_{13}$-PV peptide (ALWKTLLKKVLKAPKKKRKVC), reverse NLS peptide (ALWKTLLKKVLKAVKRKKKPC) and scrambled peptide (KTLKVAKWLKKAKPLRKLVKC) were obtained from Thermo Electron (Thermo Electron GmbH, Germany). In the reverse NLS peptide, the sequence corresponding to the nuclear localization signal of the SV40 large T antigen (aa 14–20) is inverted; the scrambled peptide was generated based on the $S4_{13}$-PV peptide sequence, so that the resulting peptide had the same amino acid composition and overall charge, but a distinct primary sequence. During synthesis, peptides were either fluorescently labeled with 5-(6)-tetramethylrhodamine (TAMRA), or modified with an acetyl group at the N-terminus, and further modified by introducing an amide group at the C-terminus. Freeze-dried peptides were reconstituted in high purity water.

Peptide concentration was determined by amino acid analysis and light absorption at 280 nm. Amino acid analysis was performed in a Beckman 6300 automatic analyzer, following acid hydrolysis of the peptide.

2.3. Peptide cellular uptake

For experiments on peptide uptake, 0.8×10^5 cells/well were seeded onto 12-well plates (flow cytometry) or 12-well plates containing 16 mm glass coverslips (confocal microscopy), 24 h prior to incubation with the peptide. The cells were then washed with phosphate-buffered saline (PBS) and incubated with 1.0 μM of either the $S4_{13}$-PV peptide or scrambled peptide, in serum-free medium, for 30 min or 1 h, at 37 °C.

Analysis of peptide internalization was performed by confocal laser scanning microscopy and flow cytometry. To avoid any possible artifactual observations caused by cell fixation, analysis of peptide uptake was performed always in live cells.

To address the effect of drugs that compromise different endocytic pathways on the uptake of the $S4_{13}$-PV peptide, HeLa cells were washed with PBS and

then pre-treated for 30 min, at 37 °C, in serum-free DMEM, with either: (i) 30 μM chlorpromazine (CHP; Sigma); (ii) 5 mM methyl-β-cyclodextrin (MβCD; Sigma); (iii) 25 μg/ml nystatin (Sigma); (iv) 5 μM cytochalasin D (Sigma); (v) 5 mM amiloride (Sigma). The cells were then incubated with the peptide in the presence of each drug, for 1 h, at 37 °C, in serum-free DMEM.

The effect of heparin on the cellular uptake of the $S4_{13}$-PV peptide was also evaluated. For this purpose, HeLa cells were washed with PBS and then pre-treated for 30 min, at 37 °C, in serum-free DMEM, with 10 μg/ml heparin (sodium salt from bovine intestinal mucosa; Sigma), followed by incubation with the peptide in the presence of heparin, for 1 h, at 37 °C, in serum-free DMEM. The concentration of heparin used in this study corresponds to a clear excess of negative charges with respect to the positive charges of the peptide, which allows to accurately mimic the interaction of the peptide with a cell surface rich in heparan sulfate proteoglycans.

The effect of the drugs that affect different endocytic pathways was confirmed, in parallel control experiments, by analyzing the cellular uptake of fluorescently labeled transferrin, a known marker of clathrin-mediated endocytosis, and lactosylceramide, a marker of raft/caveolae-dependent endocytosis (data not shown). No significant cytotoxicity was associated to the treatment of cells with any of the drugs used in this study (data not shown).

Flow cytometry analysis was performed in live cells, using a Becton Dickinson FACSCalibur flow cytometer. Data were obtained and analyzed using CellQuest software (BD Biosciences). Since flow cytometry analysis does not discriminate between membrane-associated and internalized peptide, after incubation with the different peptides, the cells were washed once with PBS and trypsinized (10 min, 37 °C) to remove any surface-bound, non-internalized peptide, which could result in an overestimation of cellular uptake. The cells were then further washed, resuspended in PBS, and immediately analyzed. Live cells were gated by forward/side scattering from a total of 10000 events.

For analysis of the subcellular localization of the peptides by confocal microscopy, following peptide–cell incubation the cells were washed and mounted in PBS, and immediately visualized. Observations were performed, in live cells, using a Bio-Rad MRC 600 fluorescence confocal microscope equipped with an argon/krypton laser (Bio-Rad Laboratories, Inc.).

2.4. Liposome preparation

Large unilamellar vesicles (LUVs) were prepared by extrusion of multilamellar vesicles composed of 1-palmitoyl-2-oleoyl-*sn*-glycero-3-phosphocholine (POPC; Avanti Polar Lipids, AL), 1-palmitoyl-2-oleoyl-*sn*-glycero-3-[phospho-*rac*-(1-glycerol)] (POPG; Avanti), or mixtures of these two lipids at different molar ratios [(POPC:POPG (1:1) and POPC:POPG (4:1)].

Lipid solutions in chloroform were mixed at the desired molar ratios, and dried under vacuum, at room temperature, using a rotary evaporator. The dried lipid films were then hydrated with 1.0 ml high purity water, and the multilamellar vesicles obtained were briefly sonicated and extruded 21 times through two stacked polycarbonate filters (100 nm pore diameter) using a Liposofast device (Avestin, Toronto, Canada).

Total lipid concentrations of the resulting LUVs were determined by the Bartlett method [20], and 10 mM stock solutions of the different liposome formulations were prepared.

2.5. Steady-state fluorescence spectroscopy

Steady-state fluorescence measurements were performed in a SPEX Fluorolog 2 spectrofluorometer, at room temperature, using 10×2 mm, or 5×5 mm quartz cuvettes.

Interaction of $S4_{13}$-PV peptide with lipid vesicles of different compositions (LUVs) was assessed by following peptide intrinsic fluorescence upon sequential addition of small volumes of concentrated vesicle stock solutions to peptide samples, up to a lipid/peptide molar ratio of 40. Experiments were performed in 10 mM sodium phosphate buffer (pH 7.0), and concentration of $S4_{13}$-PV peptide was 2.5 μM. Excitation wavelength was 280 nm and fluorescence emission was scanned from 300 to 400 nm.

All spectra were corrected for background contributions of buffer, and of different concentrations of vesicles. Spectra were not corrected for the photomultiplier wavelength dependence.

2.6. Partition coefficients

Partition coefficients (K_p) were determined based on the changes in the fluorescence intensity of the $S4_{13}$-PV peptide observed in the presence of lipid vesicles of different compositions. The relationships and assumptions used to determine K_p were previously described [21],

$$I = \frac{I_W + I_L K_p \bar{V}_L [L]}{1 + K_p \bar{V}_L [L]} \quad (1)$$

where I is the fluorescence intensity for each lipid concentration [L], and I_i the values in phase i (I=W, L). A nonlinear fit of Eq. (1) to the data yields the values of I_L and K_p. The lipid molar volume $\bar{V}_L$=0.637 $dm^3\ M^{-1}$ used in this work is obtained from extrapolation from available data in the literature [22].

2.7. Quenching of tryptophan fluorescence

Quenching of tryptophan fluorescence by acrylamide was evaluated either in aqueous buffer, or in the presence of lipid vesicles, at the lipid/peptide molar ratio of 40. Under the different experimental conditions, the quenching constants (K_{SV}) for the $S4_{13}$-PV peptide were determined by linear regression using the Stern–Volmer equation [23,24]:

$$\frac{F_0}{F} = 1 + K_{SV}[Q] \quad (2)$$

where F_0 and F are the fluorescence intensities of tryptophan emission in the absence and presence of the quencher, respectively, and [Q] is the molar concentration of the quencher in the sample.

Emission spectra of the $S4_{13}$-PV peptide (2.5 μM) were acquired as described previously, in the presence of different acrylamide concentrations (5–100 mM). Acrylamide was added from a 1.0 M aqueous stock solution. Spectra were corrected for background fluorescence of buffer, vesicles and different concentrations of acrylamide, as well as for the inner filter effect.

2.8. Circular dichroism spectroscopy

Circular dichroism (CD) spectra were acquired in a Jasco J-715 spectropolarimeter using 1.0 mm quartz cuvettes. Experiments were performed at 15 °C, in 10 mM sodium phosphate buffer (pH 7.0), or in the same buffer containing lipid vesicles, at different lipid/peptide molar ratios. Five spectra were collected and averaged for each sample. Peptide concentrations ranged from 5 to 50 μM, and maximal lipid concentration was 0.2 mM. All spectra were corrected for background contributions of buffers and lipid vesicles, and smoothed using the Jasco J-715 noise reduction software.

To facilitate interpretation of the circular dichroism spectra obtained under the different experimental conditions, the relative contribution of three secondary structure elements (α-helix, β-structure and random coil) to the overall structure of the peptide was estimated by computer fitting of the CD spectra according to the algorithm convex constraint analysis (CCA).

3. Results

3.1. Cellular uptake of $S4_{13}$-PV cell-penetrating peptide

To evaluate the efficiency of $S4_{13}$-PV peptide internalization, flow cytometry analysis of HeLa cells exposed to increasing concentrations of rhodamine-labeled peptide was performed. Enzymatic digestion of membrane-associated, non-internalized peptide prior to flow cytometry analysis ensured an accurate evaluation of peptide uptake.

Analysis of the flow cytometry results revealed that the number of cells containing the peptide and the amount of peptide internalized by cells markedly increased with peptide concentration, within the concentration range examined (Fig. 1a).

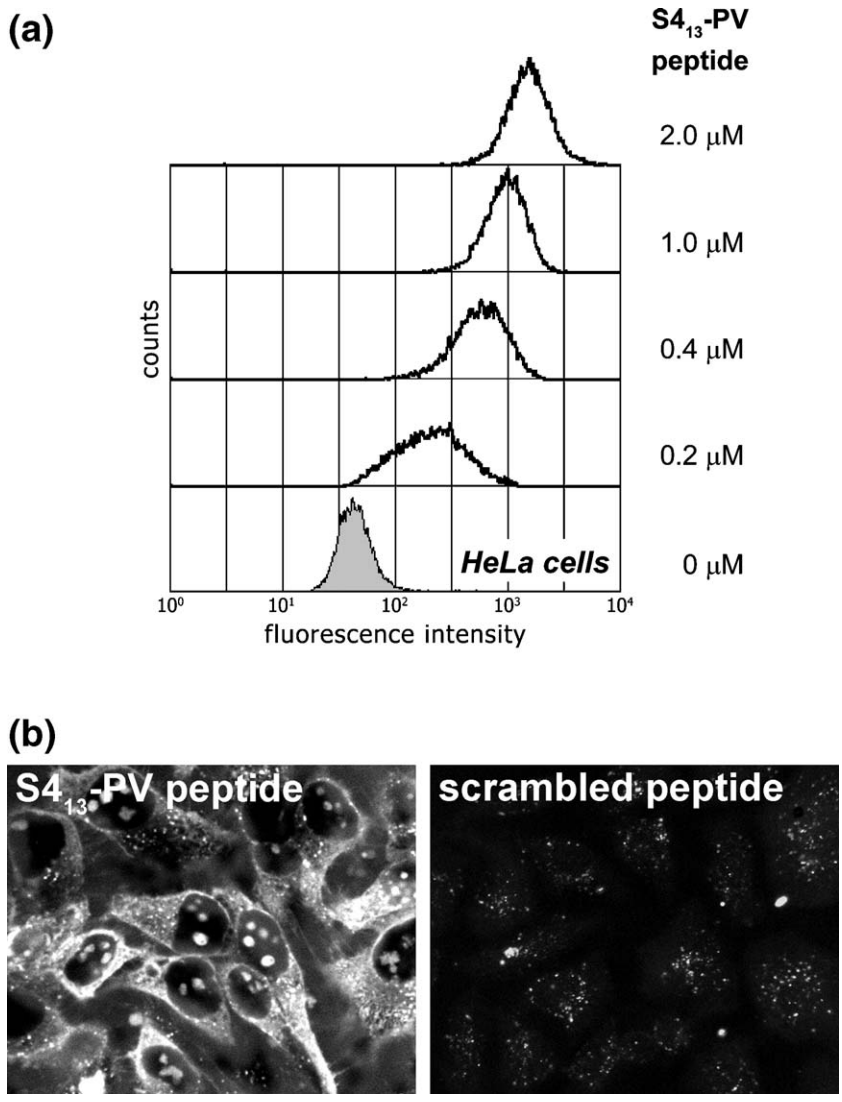

Fig. 1. Cellular uptake of $S4_{13}$-PV cell-penetrating peptide. (a) Effect of the $S4_{13}$-PV peptide dose on its cellular uptake. HeLa cells were incubated with increasing concentrations of rhodamine-labeled $S4_{13}$-PV peptide, at 37 °C, for 1 h. Extent of peptide uptake was analyzed by flow cytometry following cell treatment with trypsin, to remove non-internalized, surface-bound peptide. (b) Effect of peptide sequence on peptide uptake. HeLa cells were incubated with 1.0 μM of rhodamine-labeled $S4_{13}$-PV or scrambled peptides, at 37 °C, for 30 min. Cells were washed and immediately observed by confocal fluorescence microscopy. All experiments were performed using live cells.

Although the $S4_{13}$-PV peptide and its derivative scrambled peptide have similar physico-chemical properties (peptide length, mass and charge), the extent of cellular uptake of the $S4_{13}$-PV peptide was significantly higher than that observed for the scrambled peptide (Fig. 1b). Additionally, the two peptides presented clearly distinct subcellular localizations: the $S4_{13}$-PV peptide was distributed throughout the cytoplasm and nucleus of cells, accumulating in nucleoli, whereas the scrambled peptide presented a punctate cytoplasmic distribution, which is consistent with its uptake through an endocytic mechanism (Fig. 1b).

Additional studies aimed at evaluating the effect of the peptides on membrane integrity revealed that incubation of HeLa cells with the $S4_{13}$-PV or scrambled peptides up to 2.0 μM concentration does not result in significant cytotoxicity, as assessed by propidium iodide exclusion by viable cells ([18] and data not shown).

The different cellular uptake of the $S4_{13}$-PV and scrambled peptides highlights the relevance of peptide sequence in dictating the mechanism and efficiency of peptide uptake, which ultimately determine its intracellular fate.

3.2. Mechanisms of peptide cellular uptake

In face of recent reports demonstrating that endocytosis is responsible for the cellular uptake of several cell-penetrating peptides, the involvement of endocytosis in the cellular uptake of the $S4_{13}$-PV peptide was carefully evaluated.

Endocytosis is a very complex cellular process that may occur through several distinct mechanisms, usually divided into two broad categories: phagocytosis, a process restricted to specialized mammalian cells, and pinocytosis, which occurs in all mammalian cells and encompasses macropinocytosis, clathrin-mediated endocytosis, caveolae-mediated endocytosis,

as well as other less characterized clathrin- and caveolae-independent endocytic pathways [25,26].

To investigate the involvement of the different endocytic pathways in the cellular uptake of the $S4_{13}$-PV peptide, the effect of chlorpromazine (a known inhibitor of clathrin-mediated endocytosis), of MβCD and nystatin (which deplete or sequester membrane cholesterol, inhibiting endocytic pathways dependent on lipid-rafts such as macropinocytosis, caveolae- and clathrin-mediated endocytosis [26]), of cytochalasin D (an inhibitor of F-actin elongation required for phagocytosis, macropinocytosis and caveolar endocytosis [27]) and of amiloride (which specifically blocks the Na^+/H^+ exchange required for macropinocytosis [28]), was evaluated.

As can be observed in Fig. 2, only cytochalasin D had a significant inhibitory effect on the extent of cellular uptake of the $S4_{13}$-PV peptide, which might support a role for endocytosis in the internalization of this peptide. However, the lack of inhibition observed for all the other tested drugs, which also compromise the endocytic pathways that are affected by cytochalasin D, consistently excluded the involvement of endocytosis in the cellular uptake of the $S4_{13}$-PV peptide, at a peptide concentration that results in its efficient cellular uptake by the majority of cells (1.0 μM).

3.3. Role of heparan sulfate proteoglycans (HSPGs) in peptide uptake

As a first approach to address the involvement of cell surface heparan sulfate proteoglycans in the cellular uptake of the $S4_{13}$-PV peptide, the competitive effect of heparin on this process was evaluated. Heparin mimics the glycosaminoglycan moieties of proteoglycans ubiquitously present at cell surfaces, and has been shown to bind Tat peptide very efficiently [29] and to impair the cellular uptake of Tat fusion proteins [9,15,17,30].

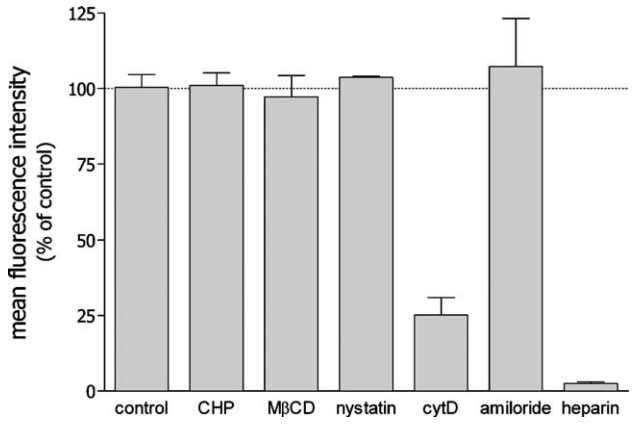

Fig. 2. Effect of different drugs on the cellular uptake of $S4_{13}$-PV peptide. Flow cytometry quantification of the extent of cellular uptake of $S4_{13}$-PV peptide in the presence of drugs that inhibit different endocytic pathways, or heparin. HeLa cells pre-treated with the different drugs for 30 min, at 37 °C, were incubated, in the presence of the drugs, with fluorescently-labeled $S4_{13}$-PV peptide (1.0 μM, 1 h), at the same temperature, as described in Materials and methods. Flow cytometry analysis was performed in live cells, following treatment with trypsin, to remove non-internalized, surface-bound peptide. Chlorpromazine (CHP) inhibits clathrin-mediated endocytosis, MβCD and nystatin inhibit endocytic pathways dependent on lipid-rafts by depleting or sequestering membrane cholesterol, cytochalasin D (cytD) inhibits F-actin elongation required for phagocytosis, macropinocytosis, caveolar endocytosis, as well as other cellular processes, and amiloride blocks the Na^+/H^+ exchange required for macropinocytosis. Heparin mimics glycosaminoglycan moieties of cell surface heparan sulphate proteoglycans.

Results from these experiments demonstrated that heparin completely blocks the cellular uptake of the $S4_{13}$-PV peptide (Fig. 2), strongly suggesting that cell surface proteoglycans play an important role in peptide–cell interaction.

To accurately evaluate the relevance of cell surface heparan sulfate proteoglycans to the interaction of the $S4_{13}$-PV peptide with biological membranes, comparative uptake studies were performed in CHO-K1 and pgs A-745 cell lines. pgs A-745 is a mutant cell line derived from CHO-K1 that is unable to synthesize proteoglycans, since it is defective in xylosyltransferase I, an enzyme involved in the early steps of glycosaminoglycan biosynthesis [31,32].

Flow cytometry analysis of the uptake of the $S4_{13}$-PV peptide by these two cell lines demonstrated that peptide uptake was more extensive in cells containing heparan sulfate proteoglycans (CHO-K1; Fig. 3a), when compared to that in mutant cells lacking proteoglycans (pgs A-745; Fig. 3b). Nonetheless, the effect of HSPGs on facilitating the cellular uptake of $S4_{13}$-PV peptide was highly dependent on peptide concentration: at low peptide concentrations, peptide uptake by cells lacking proteoglycans (pgs A-745) was approximately 10-fold lower than that by cells containing proteoglycans (CHO-K1), whereas, for higher peptide concentrations, smaller differences were observed (Fig. 3).

Overall, the results from this comparative analysis reinforce the relevance of HSPGs to the efficient cellular uptake of the $S4_{13}$-PV peptide, although the presence of these membrane components at cell surface is not mandatory.

3.4. Interaction of $S4_{13}$-PV peptide with model membranes

To characterize the interaction of the $S4_{13}$-PV peptide with membranes, a detailed analysis addressing the effect of charge density of the target membrane and of lipid/peptide ratio on the fluorescence emission spectra of the $S4_{13}$-PV peptide was performed.

Interestingly, the emission spectra of the $S4_{13}$-PV peptide remained unchanged in the presence of neutral vesicles composed of POPC, whereas upon interaction with negatively charged vesicles, clear changes in the wavelength of maximal emission of the $S4_{13}$-PV peptide towards shorter wavelengths (blue-shift) were observed, concomitantly with significant increases in fluorescence intensity (Fig. 4).

Partition coefficients (K_p), determined from the changes of peptide intrinsic fluorescence intensity observed in the presence of the different lipid vesicles, clearly indicate that the extent of peptide–membrane interaction is dependent on the surface density of negatively charged components of the target membrane (Table 2).

The shift of peptide maximal fluorescence towards shorter wavelengths (blue-shift) observed in the presence of the different negatively charged vesicles clearly indicates that,

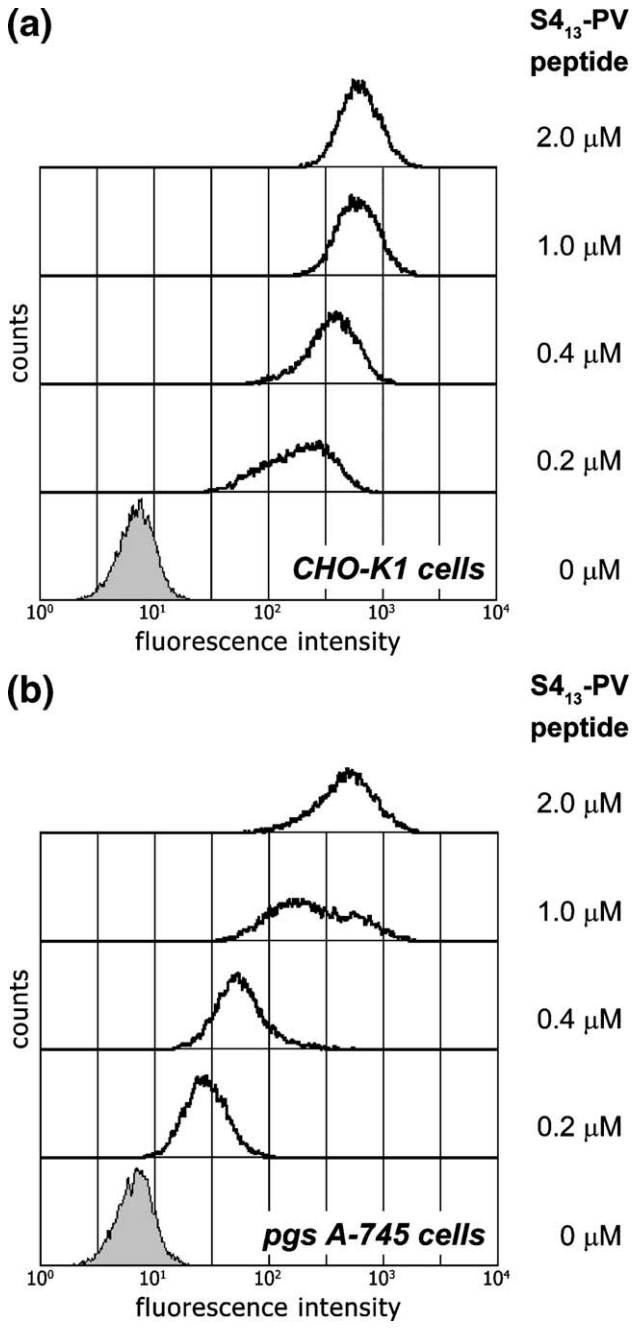

Fig. 3. Uptake of $S4_{13}$-PV peptide by cells genetically deficient in proteoglycan biosynthesis. Flow cytometry analysis of $S4_{13}$-PV peptide uptake by (a) wild-type CHO-K1 or (b) pgs A-745 cell lines. Cells were incubated with increasing concentrations of rhodamine-labeled $S4_{13}$-PV peptide, at 37 °C, for 1 h. Flow cytometry analysis was performed in live cells, following treatment with trypsin, to remove non-internalized, surface-bound peptide.

following its interaction with the vesicles, the $S4_{13}$-PV peptide becomes localized in a highly hydrophobic environment. Interestingly, the magnitude of the blue-shift of maximal fluorescence emission of the $S4_{13}$-PV peptide induced by the negatively charged vesicles increased with the charge density of target membranes (POPC:POPG (4:1)<POPC:POPG (1:1)<POPG), as well as with lipid/peptide ratio (Fig. 4; Table 2). As expected, with increasing lipid/peptide ratios, the difference between the magnitudes of the blue-shifts induced by the different negatively charged vesicles was progressively less pronounced, the shifts being comparable at lipid/peptide ratios of 40, or higher (Fig. 4b; Table 2).

In agreement with the lack of interaction between the $S4_{13}$-PV peptide and neutral membranes, quenching values of intrinsic fluorescence of the $S4_{13}$-PV peptide by acrylamide in the presence of lipid vesicles composed of POPC were comparable to those of the peptide in buffer (as evaluated by the corresponding K_{SV}; Table 2), indicating that the $S4_{13}$-PV peptide remains completely exposed to the aqueous environment in the presence of these vesicles. Conversely, following interaction of the $S4_{13}$-PV with the different negatively charged

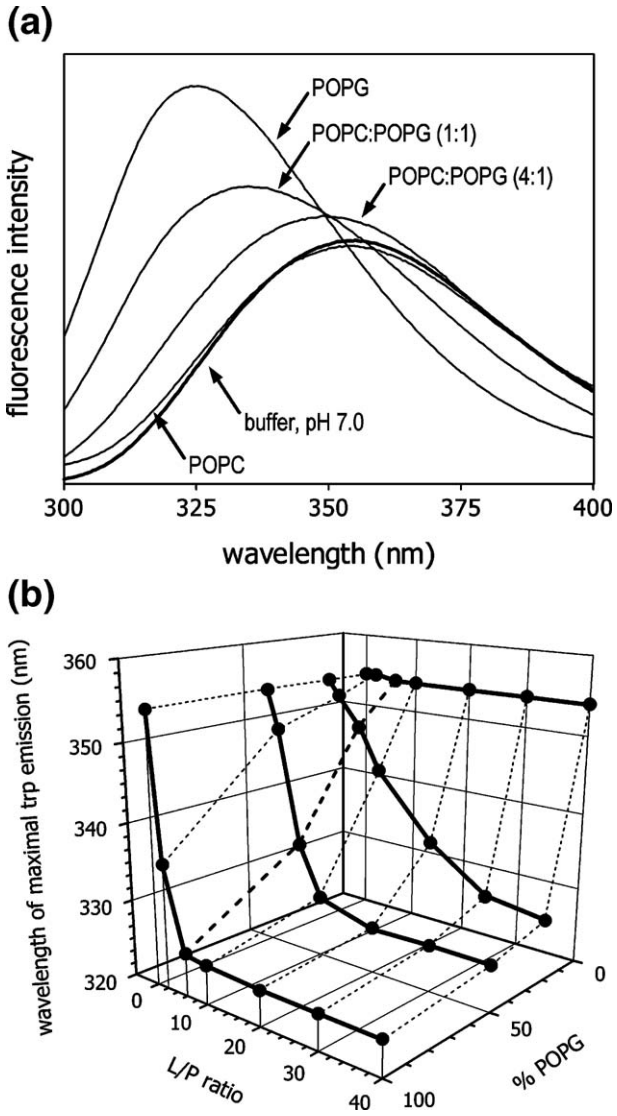

Fig. 4. Intrinsic fluorescence of the $S4_{13}$-PV peptide in the presence of model membranes. (a) Effect of target membrane phospholipid composition. Spectra were acquired in sodium phosphate buffer, pH 7.0, and in the presence of neutral vesicles composed of POPC or negatively charged vesicles composed of POPC:POPG (4:1), POPC:POPG (1:1), or POPG, at a lipid/peptide ratio of 6. (b) Effect of target membrane phospholipid composition and lipid/peptide ratio on the wavelength of maximal intrinsic fluorescence emission of the $S4_{13}$-PV peptide. Results obtained at a lipid/peptide ratio of 6 are highlighted. Excitation wavelength was 280 nm and fluorescence emission was scanned from 300 to 400 nm.

Table 2
Biophysical characterization of the interaction of $S4_{13}$-PV cell-penetrating peptide with target membranes of different phospholipid composition

	K_p ($\times 10^5$)	λ_{max} (nm)	$\Delta\lambda_{max}$ (nm)	K_{SV} (M^{-1})
$S4_{13}$-PV peptide				
buffer, pH 7.0	–	354	–	15.7±0.3
POPC	n.d.	354	0	14.8±0.7
POPC:POPG (4:1)	0.23±0.1	328	26	2.3±0.2
POPC:POPG (1:1)	1.17±0.4	326	28	2.1±0.1
POPG	1.96±0.6	324	30	3.1±0.2

K_p values were determined by non-linear regression fitting using Eq. (1); K_{SV} were determined by fitting Eq. (2) to experimental data; values of λ_{max}, $\Delta\lambda_{max}$ and K_{SV} obtained in the presence of lipid vesicles correspond to a lipid/peptide ratio of 40.

vesicles, a significant decrease in the efficiencies of fluorescence quenching by acrylamide were observed, regardless of the density of negatively charged phospholipids in the target membranes (K_{SV}; Table 2).

Since the Stern–Volmer constants (K_{SV}) in Table 2, are the product of the bimolecular quenching rate constant times the fluorescence lifetime, and the quantum yields and lifetimes increase upon interaction of the peptide with the membranes, the significant decrease of K_{SV} observed in the presence of negatively charged membranes are a consequence of the shielding of the tryptophan to the aqueous environment, and thereby to the acrylamide quencher.

These results are in agreement with those described to above regarding the spectral changes of the $S4_{13}$-PV peptide, which collectively demonstrate that the $S4_{13}$-PV peptide, or at least the region of the peptide that contains the tryptophan residue, becomes less exposed to the aqueous environment, most likely buried into the lipid bilayer, as a consequence of its interaction with negatively charged membranes.

3.5. $S4_{13}$-PV peptide conformational changes induced by target membranes

To determine whether the interaction of the $S4_{13}$-PV peptide with membranes would result in changes of peptide conformation, circular dichroism experiments were performed in the presence of lipid vesicles of different compositions (neutral POPC vesicles, and negatively charged POPC:POPG (1:1) or POPG vesicles).

Analysis of circular dichroism spectra of the $S4_{13}$-PV peptide in buffer clearly demonstrated that, when free in aqueous solution, the peptide is completely unstructured (Fig. 5). Interestingly, the CD spectra of the $S4_{13}$-PV peptide in the presence of vesicles composed of POPC was virtually indistinguishable from that obtained in buffer, demonstrating that no peptide conformational changes are induced by neutral membranes, even at high lipid/peptide ratios (Fig. 5).

In contrast, prominent changes in the secondary structure of the $S4_{13}$-PV peptide were observed in the presence of vesicles containing negatively charged phospholipids (Fig. 5). In agreement with the changes in the intrinsic fluorescence of the $S4_{13}$-PV peptide observed previously, the extent of peptide conformational changes induced by the different vesicles was highly dependent on membrane charge density (compare the results obtained in the presence of vesicles composed of POPG or POPC:POPG (1:1) at a lipid/peptide ratio of 4), as well as on the lipid/peptide ratio (exemplified by the peptide conformational changes induced by POPC:POPG (1:1) vesicles at lipid/peptide ratios of 4 and 8). Analysis of the obtained CD spectra indicates that the changes in peptide conformation induced by the different negatively charged vesicles are consistent with an increase in the contribution of an alpha-helical structural component, and in some cases also of a beta structural component.

To elucidate whether the $S4_{13}$-PV peptide secondary structure induced by the negatively charged membranes is a consequence of specific peptide–membrane interactions, or rather the outcome of non-specific interactions of electrostatic nature, and to analyze the relevance of the two components of the $S4_{13}$-PV fusion peptide to this process, parallel circular dichroism experiments were performed using the reverse NLS and scrambled peptides.

Similarly to what was previously observed for the $S4_{13}$-PV peptide, analysis of the CD spectra of the reverse NLS and scrambled peptides clearly showed that these peptides are completely unstructured in aqueous buffer (Fig. 6). Nonetheless, the conformational changes of the scrambled peptide, induced upon its interaction with negatively charged membranes composed of POPG, were significantly less pronounced than those observed for the $S4_{13}$-PV and reverse NLS peptides, and no increase of an alpha-helical structural component was detected (Fig. 6).

Given the similar physico-chemical properties of the $S4_{13}$-PV, reverse NLS and scrambled peptides (peptide length, mass

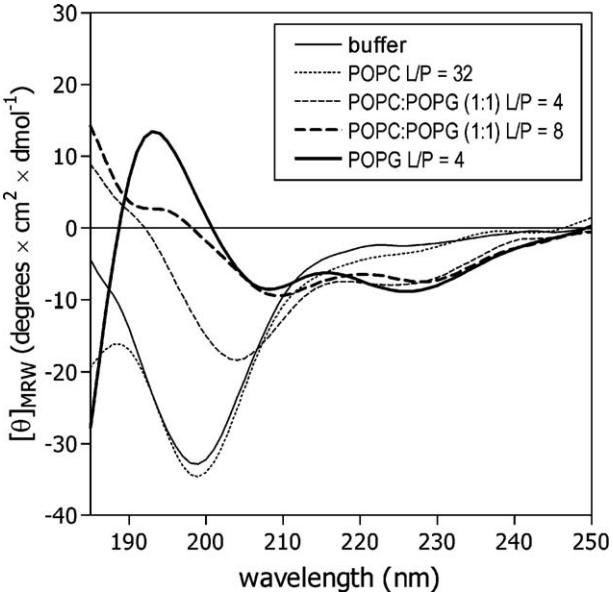

Fig. 5. Circular dichroism analysis of conformational changes of $S4_{13}$-PV peptide in the presence of model membranes. Circular dichroism spectra of $S4_{13}$-PV peptide were acquired in sodium phosphate buffer, pH 7.0, or in the presence of neutral target membranes composed of POPC, or negatively charged vesicles composed of POPC:POPG (1:1), or POPG, at the indicated lipid/peptide ratios, as described in Materials and methods.

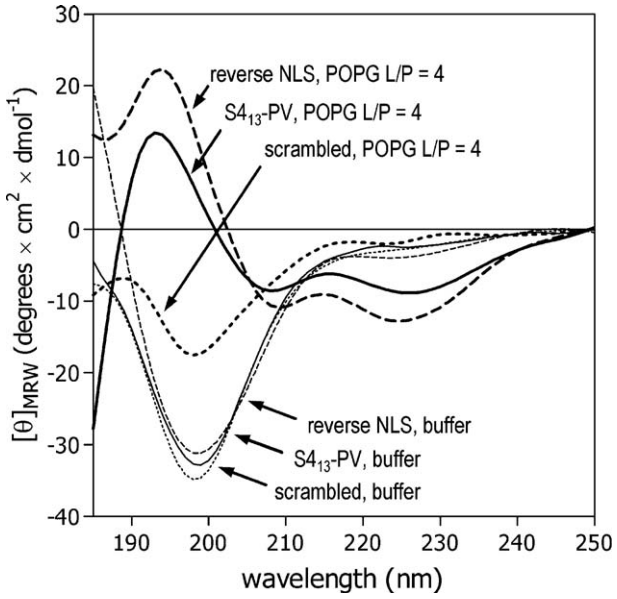

Fig. 6. Effect of peptide sequence on the conformational changes induced by interaction with negatively charged membranes. Circular dichroism spectra of $S4_{13}$-PV, reverse NLS and scrambled peptides were acquired in sodium phosphate buffer, pH 7.0, or in the presence of negatively charged vesicles composed of POPG, at a lipid/peptide ratio of 4, as described in Materials and methods.

and charge), and the identical propensities of these peptides to form alpha-helical structures, as evaluated by CD experiments performed in trifluoroethanol (TFE), an apolar, "membrane-mimicking" solvent (data not shown), the distinct behavior of the peptides observed in the presence of negatively charged vesicles clearly demonstrates that the conformational changes induced by target membranes are highly dependent on peptide sequence. Moreover, these findings demonstrate that the sequence derived from the Dermaseptin S4 peptide, which corresponds to aa 1–13 of the $S4_{13}$-PV and reverse NLS peptides, is required for the formation of a helical structure.

4. Discussion

Accumulated reports demonstrating that the cellular uptake of some cell-penetrating peptides occurs through endocytosis, or is a consequence of artifacts caused by cell fixation, prompted the re-evaluation of the mechanism involved in the cellular uptake of the Dermaseptin-derived $S4_{13}$-PV cell-penetrating peptide.

In this context, the possible involvement of endocytosis in the cellular uptake of the $S4_{13}$-PV peptide was investigated by analyzing the extent of peptide uptake in the presence of drugs that selectively compromise different endocytic pathways. Results demonstrating that the uptake of the $S4_{13}$-PV peptide occurs through a very efficient, non-toxic and dose dependent mechanism, together with the observations that, among all the tested drugs, only cytochalasin D had an inhibitory effect on the cellular uptake of the $S4_{13}$-PV peptide, excluded the involvement of endocytosis as the mechanism responsible for the efficient cellular uptake of the $S4_{13}$-PV peptide. Additional observations showing that cellular uptake of the $S4_{13}$-PV peptide was not inhibited upon cell treatment with metabolic inhibitors that non-specifically block all endocytic pathways (sodium azide, sodium fluoride, antimycin A; unpublished observations), as well as the diffuse rather than punctated intracellular distribution of the peptide, reinforce the lack of involvement of endocytosis in the cellular uptake of this peptide.

Although the results from experiments performed at lower peptide concentrations (0.2 μM and 0.4 μM) demonstrated the involvement of the clathrin-mediated pathway of endocytosis in the cellular uptake of the $S4_{13}$-PV peptide [18], it should be emphasized that at peptide concentrations leading to efficient uptake of the peptide by the majority of cells (1.0 μM), the involvement of an endocytosis-independent mechanism of uptake is clearly prevalent.

The dramatic inhibition of cellular uptake of the $S4_{13}$-PV peptide by heparin, which mimics GAG moieties of heparan sulfate proteoglycans ubiquitously present at cell surfaces, strongly suggests that the interactions between the positively charged peptide and highly negatively charged membrane components play an important role in the overall process of cellular uptake of the peptide.

More interestingly, comparative analysis of peptide uptake by normal and genetically modified cells that are deficient in proteoglycan biosynthesis clearly demonstrated that heparan sulfate proteoglycans potentiate the cellular uptake of the $S4_{13}$-PV peptide. This effect is particularly relevant for low peptide concentrations, most likely because binding of the peptide to cell membranes is not a limiting step to the cellular uptake at high peptide concentrations. Nonetheless, and in contrast with previous reports showing that heparan sulfate proteoglycans are absolutely required for the cellular uptake of full length tat and tat-fusion proteins [9,10,33], the presence of HSPGs at cell surface is not mandatory for the cellular uptake of the $S4_{13}$-PV peptide.

Moreover, the results obtained indicate that binding of the $S4_{13}$-PV peptide to cell membranes, which is facilitated by interaction with cell surface HSPGs, can either result in the endocytic uptake of the peptide (as discussed above for experiments performed at low $S4_{13}$-PV peptide concentrations), or evoke conformational changes in the peptide, which occur concomitantly with its insertion into the membrane leading to its efficient uptake by the majority of cells.

The data demonstrating that the main mechanism responsible for the cellular uptake of the $S4_{13}$-PV cell-penetrating peptide is distinct from endocytosis and is facilitated by the presence of negatively charged proteoglycans at cell surface indicate that the membrane translocation of the $S4_{13}$-PV cell-penetrating peptide results from its direct interaction with biological membranes. Aiming at gaining insights into the molecular mechanisms underlying the translocation of the $S4_{13}$-PV peptide across biological membranes, a detailed characterization of the interaction of the $S4_{13}$-PV peptide with model membranes was performed.

In agreement with the role of proteoglycans in facilitating peptide uptake, analysis of the interaction of the $S4_{13}$-PV peptide with target membranes of different phospholipid compositions clearly demonstrated that the extent of peptide–membrane interactions is dependent on the relative amount of negatively charged membrane components on the target membrane. Although these results indicate that the interactions established between the $S4_{13}$-PV peptide and target membranes are essentially of electrostatic nature, the interaction of the peptide with cell surface proteoglycans may involve some structural recognition.

As a consequence of the interaction of the $S4_{13}$-PV peptide with negatively charged target membranes, significant changes in the intrinsic fluorescence spectra of the peptide were detected, namely an increase in the fluorescence intensity and a shift of the wavelength of maximal emission towards shorter wavelengths (blue-shift). These spectral changes, which are indicative of an increase in the hydrophobicity of the peptide environment, were dependent both on the density of negatively charged phospholipids in the target membrane and on the lipid/peptide ratio. Remarkably, the magnitude of the blue-shifts induced upon interaction of the $S4_{13}$-PV peptide with negatively charged membranes, at the lipid/peptide ratio of 40 (30 nm in the case of POPG vesicles), is extremely high, specially when compared to those previously reported for other CPPs, such as the Penetratin, Transportan or Pep-1 peptides, for which lower shifts were observed [34–37].

In agreement with these changes of peptide intrinsic fluorescence, the Stern–Volmer quenching constants (K_{SV}) calculated in the presence of the different negatively charged vesicles undoubtedly demonstrated that the $S4_{13}$-PV peptide, or at least the region of the peptide that contains the tryptophan residue, becomes localized into an extremely hydrophobic environment as a consequence of its interaction with negatively charged membranes, most likely inserted into the lipid bilayer.

Concomitantly with the spectral changes described previously, circular dichroism analysis revealed that the interaction of the $S4_{13}$-PV peptide with the negatively charged vesicles used in this study also induced significant peptide conformational changes, consistent with an increase in the helical content of the peptide, whose extent was dependent on the density of negatively charged phospholipids in the target membrane, as well as on the lipid/peptide ratio. The similar dependences observed for the magnitude of the spectral changes and the extent of peptide conformational changes strongly suggest that the latter are intricately associated to the insertion of the $S4_{13}$-PV peptide into target membranes, and presumably to its ability to translocate across biological membranes.

In this context, it is noteworthy that significant differences were observed between the conformational changes of the $S4_{13}$-PV and reverse NLS peptides, induced upon their interaction with negatively charged target membranes, and those of the scrambled peptide. This distinct behavior highlights the importance of the sequence derived from the Dermaseptin S4 peptide to the formation of the alpha-helical structure resulting from the interaction of the $S4_{13}$-PV peptide with negatively charged membranes. Moreover, these data strongly indicate that such conformational changes are of critical importance for the increased capacity exhibited by the $S4_{13}$-PV peptide to translocate across biological membranes, as compared to the scrambled peptide. Interestingly, in contrast to the scrambled peptide, the amino acids 1–13 of the $S4_{13}$-PV and reverse NLS peptides, which were originally derived from the Dermaseptin peptide, have the capacity to be arranged as an amphipathic α-helix (Fig. 7). Although this feature is not a requirement for peptide translocation across membranes, the importance of these structural motifs in inducing local membrane destabilization, which can be crucial for peptide translocation, should not be neglected.

Overall, the results reviewed in the present study demonstrate that the main mechanism involved in the cellular uptake of the $S4_{13}$-PV peptide, which is distinct from endocytosis, can be rationalized in several distinct steps. The process is initiated by the binding of the $S4_{13}$-PV cell-penetrating peptide to membranes, as a consequence of electrostatic interactions established with negatively charged membrane components, such as the highly negatively charged cell surface heparan sulfate proteoglycans, in the case of cell membranes. As a consequence of peptide–membrane interactions that occur upon binding to target membranes, the $S4_{13}$-PV peptide becomes inserted into the lipid bilayer, which occurs concomitantly with significant conformational changes of the peptide that result in the formation of an amphipathic α-helix. Whether these conformational changes constitute a requirement for the insertion of the $S4_{13}$-PV peptide into the lipid bilayer, or a consequence of this process, is not clear. In any case, the translocation of the peptide to the intracellular milieu is, most likely, a consequence of a transient and confined membrane destabilization induced by the amphipathic α-helix that is formed upon peptide–membrane interaction. Based on recent reports demonstrating that the transbilayer membrane potential that exists across cell membranes (negative inside) is required

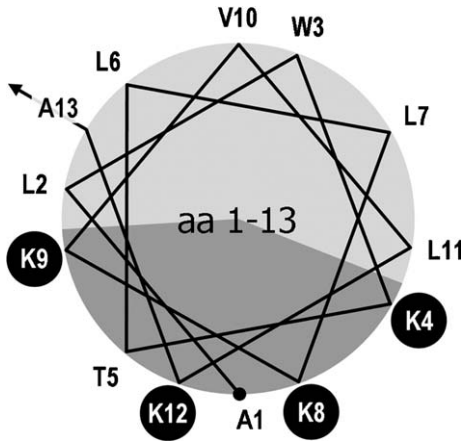

Fig. 7. Helical plot representation of the $S4_{13}$-PV cell-penetrating peptide. Only the amino acids 1–13, which are derived from the Dermaseptin peptide, are plotted. Most likely, the sequence corresponding to the NLS of SV40 remains unstructured due to repulsion forces between positively charged residues. Hydrophilic amino acids are shown in black.

for the cellular uptake of several cell-penetrating peptides [38–40], the possibility that the membrane potential also acts as a driving force for the membrane translocation of the $S4_{13}$-PV peptide should not be excluded.

Studies are currently in progress in our laboratory aiming at evaluating the potential of the $S4_{13}$-PV cell-penetrating peptide to mediate the intracellular delivery of molecules of pharmacological interest, including drugs, proteins and nucleic acids.

Acknowledgements

We thank Prof. F. Regateiro, Head of the Centro de Histocompatibilidade de Coimbra (Portugal), for scientific collaboration in this study. This study was supported by a grant from the Portuguese Foundation for Science and Technology (POCTI/CVT/44854/2002). M. Mano is recipient of a fellowship from the Portuguese Foundation for Science and Technology.

References

[1] U. Langel, Cell Penetrating Peptides: Processes and Applications, CRC Press, Boca Raton, FL, 2002.
[2] M. Magzoub, A. Graslund, Cell-penetrating peptides: small from inception to application, Q. Rev. Biophys. 37 (2004) 147–195.
[3] A. Joliot, A. Prochiantz, Transduction peptides: from technology to physiology, Nat. Cell Biol. 6 (2004) 189–196.
[4] E.L. Snyder, S.F. Dowdy, Cell penetrating peptides in drug delivery, Pharm. Res. 21 (2004) 389–393.
[5] S. Deshayes, M.C. Morris, G. Divita, F. Heitz, Cell-penetrating peptides: tools for intracellular delivery of therapeutics, Cell Mol. Life Sci. 62 (2005) 1839–1849.
[6] E. Vives, P. Brodin, B. Lebleu, A truncated HIV-1 Tat protein basic domain rapidly translocates through the plasma membrane and accumulates in the cell nucleus, J. Biol. Chem. 272 (1997) 16010–16017.
[7] D. Derossi, A.H. Joliot, G. Chassaing, A. Prochiantz, The third helix of the Antennapedia homeodomain translocates through biological membranes, J. Biol. Chem. 269 (1994) 10444–10450.
[8] M.C. Morris, J. Depollier, J. Mery, F. Heitz, G. Divita, A peptide carrier for the delivery of biologically active proteins into mammalian cells, Nat. Biotechnol. 19 (2001) 1173–1176.
[9] M. Tyagi, M. Rusnati, M. Presta, M. Giacca, Internalization of HIV-1 tat requires cell surface heparan sulfate proteoglycans, J. Biol. Chem. 276 (2001) 3254–3261.
[10] J.P. Richard, K. Melikov, H. Brooks, P. Prevot, B. Lebleu, L.V. Chernomordik, Cellular uptake of unconjugated TAT peptide involves clathrin-dependent endocytosis and heparan sulfate receptors, J. Biol. Chem. 280 (2005) 15300–15306.
[11] M. Lundberg, S. Wikstrom, M. Johansson, Cell surface adherence and endocytosis of protein transduction domains, Mol. Ther. 8 (2003) 143–150.
[12] J.P. Richard, K. Melikov, E. Vives, C. Ramos, B. Verbeure, M.J. Gait, L. V. Chernomordik, B. Lebleu, Cell-penetrating peptides. A reevaluation of the mechanism of cellular uptake, J. Biol. Chem. 278 (2003) 585–590.
[13] E. Vives, J.P. Richard, C. Rispal, B. Lebleu, TAT peptide internalization: seeking the mechanism of entry, Curr. Protein Pept. Sci. 4 (2003) 125–132.
[14] M.E. Ferrari, C.M. Nguyen, O. Zelphati, Y.L. Tsai, P.L. Felgner, Analytical methods for the characterization of cationic lipid nucleic acid complexes, Hum. Gene Ther. 9 (1998) 341–351.
[15] A. Fittipaldi, A. Ferrari, M. Zoppe, C. Arcangeli, V. Pellegrini, F. Beltram, M. Giacca, Cell membrane lipid rafts mediate caveolar endocytosis of HIV-1 Tat fusion proteins, J. Biol. Chem. 278 (2003) 34141–34149.
[16] I.M. Kaplan, J.S. Wadia, S.F. Dowdy, Cationic TAT peptide transduction domain enters cells by macropinocytosis, J. Control. Release 102 (2005) 247–253.
[17] J.S. Wadia, R.V. Stan, S.F. Dowdy, Transducible TAT-HA fusogenic peptide enhances escape of TAT-fusion proteins after lipid raft macropinocytosis, Nat. Med. 10 (2004) 310–315.
[18] M. Mano, C. Teodosio, A. Paiva, S. Simoes, M.C. Pedroso de Lima, On the mechanisms of the internalization of $S4_{13}$-PV cell penetrating peptide, Biochem. J. 390 (2005) 603–612.
[19] E. Hariton-Gazal, R. Feder, A. Mor, A. Graessmann, W. Brack, D. Jans, C. Gilon, A. Loyter, Targeting of nonkaryophilic cell-permeable peptides into the nuclei of intact cells by covalently attached nuclear localization signals, Biochemistry 41 (2002) 9208–9214.
[20] G.R. Bartlett, Phosphorus assay in column chromatography, J. Biol. Chem. 234 (1959) 466–468.
[21] N.C. Santos, M. Prieto, M.A. Castanho, Quantifying molecular partition into model systems of biomembranes: an emphasis on optical spectroscopic methods, Biochim. Biophys. Acta 1612 (2003) 123–135.
[22] D. Marsh, CRC Handbook of Lipid Bilayers, CRC Press, Boca Raton, FL, 1990.
[23] A.I. De Kroon, M.W. Soekarjo, J. De Gier, B. De Kruijff, The role of charge and hydrophobicity in peptide–lipid interaction: a comparative study based on tryptophan fluorescence measurements combined with the use of aqueous and hydrophobic quenchers, Biochemistry 29 (1990) 8229–8240.
[24] J.R. Lakowicz, Principles of Fluorescence Spectroscopy, 2nd ed., Kluwer Academic/Plenum Publishers, New York, NY, 1999.
[25] S.D. Conner, S.L. Schmid, Regulated portals of entry into the cell, Nature 422 (2003) 37–44.
[26] B.J. Nichols, J. Lippincott-Schwartz, Endocytosis without clathrin coats, Trends Cell Biol. 11 (2001) 406–412.
[27] P. Sampath, T.D. Pollard, Effects of cytochalasin, phalloidin, and pH on the elongation of actin filaments, Biochemistry 30 (1991) 1973–1980.
[28] M.A. West, M.S. Bretscher, C. Watts, Distinct endocytotic pathways in epidermal growth factor-stimulated human carcinoma A431 cells, J. Cell Biol. 109 (1989) 2731–2739.
[29] S. Hakansson, A. Jacobs, M. Caffrey, Heparin binding by the HIV-1 tat protein transduction domain, Protein Sci. 10 (2001) 2138–2139.
[30] M. Rusnati, D. Coltrini, P. Oreste, G. Zoppetti, A. Albini, D. Noonan, D. Adda, M. Giacca, M. Presta, Interaction of HIV-1 Tat protein with heparin. Role of the backbone structure, sulfation, and size, J. Biol. Chem. 272 (1997) 11313–11320.
[31] J.D. Esko, T.E. Stewart, W.H. Taylor, Animal cell mutants defective in glycosaminoglycan biosynthesis, Proc. Natl. Acad. Sci. U. S. A. 82 (1985) 3197–3201.
[32] J.D. Esko, A. Elgavish, T. Prasthofer, W.H. Taylor, J.L. Weinke, Sulfate transport-deficient mutants of Chinese hamster ovary cells. Sulfation of glycosaminoglycans dependent on cysteine, J. Biol. Chem. 261 (1986) 15725–15733.
[33] M. Silhol, M. Tyagi, M. Giacca, B. Lebleu, E. Vives, Different mechanisms for cellular internalization of the HIV-1 Tat-derived cell penetrating peptide and recombinant proteins fused to Tat, Eur. J. Biochem. 269 (2002) 494–501.
[34] M. Magzoub, K. Kilk, L.E. Eriksson, U. Langel, A. Graslund, Interaction and structure induction of cell-penetrating peptides in the presence of phospholipid vesicles, Biochim. Biophys. Acta 1512 (2001) 77–89.
[35] M. Magzoub, L.E. Eriksson, A. Graslund, Comparison of the interaction, positioning, structure induction and membrane perturbation of cell-penetrating peptides and non-translocating variants with phospholipid vesicles, Biophys. Chem. 103 (2003) 271–288.
[36] P.E. Thoren, D. Persson, E.K. Esbjorner, M. Goksor, P. Lincoln, B. Norden, Membrane binding and translocation of cell-penetrating peptides, Biochemistry 43 (2004) 471–3489.
[37] S. Deshayes, A. Heitz, M.C. Morris, P. Charnet, G. Divita, F. Heitz, Insight into the mechanism of internalization of the cell-penetrating carrier peptide

Pep-1 through conformational analysis, Biochemistry 43 (2004) 1449–1457.
[38] D. Terrone, S.L. Sang, L. Roudaia, J.R. Silvius, Penetratin and related cell-penetrating cationic peptides can translocate across lipid bilayers in the presence of a transbilayer potential, Biochemistry 42 (2003) 13787–13799.
[39] S.T. Henriques, M.A. Castanho, Consequences of nonlytic membrane perturbation to the translocation of the cell penetrating peptide pep-1 in lipidic vesicles, Biochemistry 43 (2004) 9716–9724.
[40] J.B. Rothbard, T.C. Jessop, P.A. Wender, Adaptive translocation: the role of hydrogen bonding and membrane potential in the uptake of guanidinium-rich transporters into cells, Adv. Drug. Deliv. Rev. 57 (2005) 495–504.